

# The Fractal Structure of Matter and the Casimir Effect

Daniele Funaro

Department of Mathematics  
University of Modena and Reggio Emilia  
Via Campi 213/B, 41125 Modena (Italy)  
daniele.funaro@unimore.it

## Abstract

The zero-point radiation is an electromagnetic form of energy pervading the universe. Its existence is granted by standard quantum theories. We provide here an explanation based on deterministic classical electrodynamics, by associating to particles and nuclei a series of shells, made of constrained photons, with frequencies decaying with the distance. Such photons are part of a pre-existing background, evolving in vacuum even at zero temperature, and are captured by stable subatomic particles to form very distinctive quantized patterns. The evolving shells bring, for instance, to the creation of a fractal-type structure of electromagnetic layers around a conductive body. This property is then used to justify, both qualitatively and quantitatively, the attractive Casimir force of two metal plates. The analysis is carried out by standard arguments, except that here the surrounding zero-point energy is finite and, albeit with a very complicated appearance, very well-organized.

Keywords: fractals, Casimir effect, photon, electromagnetism, zero-point energy.

PACS: 33.80.-b Photon interactions with molecules; 42.50.Lc Quantum fluctuations, quantum noise, and quantum jumps; 61.43.Hv Fractals, macroscopic aggregates.

## 1 A huge electromagnetic background

The results of this paper are consequential to those collected in [17], where a throughout revision of the theory of electromagnetism in vacuum has been presented. In that book, a set of model equations, combining classical electromagnetism with Euler's equation for (immaterial) fluids, are discussed. The new model allows for the treatment of an immense variety of electromagnetic phenomena, by prescribing the exact evolution of the fields in a very wide context. The theory is imbedded in the general relativity framework with the help

of Einstein's equation. In this way, the local metric turns out to be both cause and effect in the dynamical process. As a matter of fact, the geometry is generated by the electromagnetic environment, but, at the same time, it drives the wave itself along geodesics paths, giving stability to such a coupled system. We review very quickly the main consequences of this approach and we report at the end of this section the equations, as they are formulated in a flat metric space. Of course, the reader interested to know more about the model, both quantitatively and qualitatively, can find the full set of equations and the discussion of their properties in [17].

A first interesting subset of solutions that can be examined is the one containing *free-waves*. These are solitary travelling waves, evolving according to the standard rules of geometrical optics. Unperturbed photons with compact support and perfect spherical waves belong for instance to this category. The space-time geometry is mildly modified in this case and has no influence on the natural development of the wave-fronts. The most of the electromagnetic emissions belong however to the class of *constrained waves*, in which the interaction of different solitons is allowed.

The simplest configuration associated with constrained waves is the energetically isolated system consisting of two or more rotating photons, producing a dynamic configuration in stable equilibrium. Such a motion generates a distortion of the space-time, via Einstein's equation, and the arrangement is expected to be stable when the photons actually follow the geodesics of the so deformed geometry. Explicit solutions can be computed in the 2-D case (see also the movies in [18]). At each point, the electric vector field oscillates, communicating the vibrations to the neighboring points. The global information travels along circles giving the idea of a rotating disk. Such turning photons can also carry a charge and generate a gravitational setting as a consequence of the deformation of the geometry. The frequency of rotation is inversely proportional to the magnitude of the disk (according to the intuition that small bodies are related to high frequencies, and viceversa).

These objects have a finite measure, which is dictated by the compensation properties of the space-time geometry. In fact, if one imposes that photons must travel at the speed of light also in a rotating setting, the clock has to be continuously adjusted as it moves radially. One can verify from the available exact solutions that, for a certain radius, the oscillations of the electric field  $\mathbf{E}$  (see (1.1)-(1.4)) are lined up with the direction of motion  $\mathbf{V}$  of the wave. This is the action limit of the metric and, compatibly with the model equations, it can be taken as a physical boundary. Going beyond such a boundary would bring to a peripheral velocity too large to be compensated by the metric. This is a first sign of quantization, although quantum phenomena are not directly imprinted in the model equations, but they only show up in presence of special solutions (such as the ones we are now discussing).

The 3-D version of the rotating photons displays a toroid shape and has a straightforward relation with fluid dynamics vortex rings, which are known to be very stable entities. For this reason, in [17], the possibility that stable

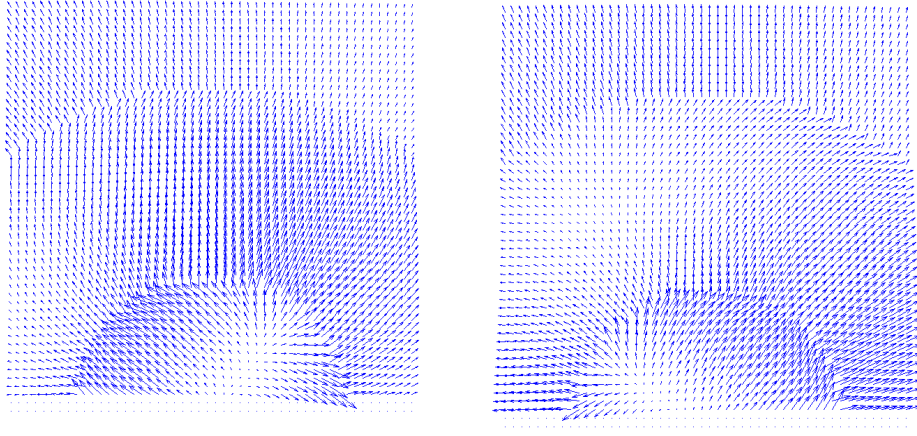


Figure 1: Quantized electric vector fields around a 2-D elementary particle at different phases of evolution. The information travels clockwise, but the angular velocity is lower as one moves from the center. In this way, the angular momentum is preserved.

elementary particles (such as the electron) could be made of rotating waves, constrained in tiny regions of space, has been taken into consideration. We do not insist further on this aspect, since here it is not relevant for the developments we have in mind. We are more concerned with a secondary effect: when some electromagnetic energy is present around a spinning particle (whatever its structure is), a sequence of layers may develop. Then, the core of the particle turns out to be surrounded by numerous concentric shells, consisting of photons rotating at different frequencies. The fluid dynamics equivalent is a kind of tornado (see [8], in order to have an idea on how this can be actually realized in a 3-D environment). The angular velocity diminishes as the respective shell becomes larger and larger. Again, the diameter of the shells is controlled by the space-time metric. This quantum-like mechanism, allows for the diffusion of the electric charge to the whole space (see also section 5).

We provide a qualitative example in figure 1 (see also the animation in [18]), where part of a central kernel and two contiguous shells are oscillating at different regimes. The displayed vectors are related to the electric field  $\mathbf{E}$  (the magnetic field  $\mathbf{B}$  is orthogonal to the page). With the exception of the most inner part, having nonzero constant charge density, the intensity of the vectors decays as the square of the distance from the center, while they oscillate with a frequency that reduces with the distance. More precisely, there is a radial stationary continuous component decaying at infinity (as classically assumed), perturbed by quantized zero-average oscillations. The vectors do not actually translate, but they carry information along closed orbits following the geodesics of a curved space-time. Based on the results in [17] the movement is necessary in order to “activate” the tensor at the right-hand side of the Einstein’s equation,

so that producing a non flat geometry (associated to the same curved geodesics followed by the photons). It can be shown in fact that stationary solutions do not deform the geometry in the appropriate way and bring to unwanted point-wise singularities.

Two oscillating layers are divided by a separation surface and the information travels at different speeds on both sides. Nevertheless, no discontinuities are actually measured. First of all, according to the model equations (see (1.4)), this is true because the velocities, independently on both sides, follow the rules of inviscid fluid dynamics. Secondly, the space-time geometry is deformed in such a way that, after writing the electromagnetic constitutive equations in the new metric, there are no derivatives to be computed in a direction transversal to the separation surface. The central core and the successive shells are independent entities that do not communicate directly, but only through slight vibrations of the separation surfaces, around the position of equilibrium (as it happens in any perturbed mechanical system). Discontinuities are consequence of the wrong idea that such a complicated phenomenon can be actually explained from the framework of a flat geometry. A characterization of a separation surface is obtained by observing that the derivative with respect to time of the electric field is tangent to it, i.e., the time-dependent component of the field, orthogonal to the surface, is zero. This brings to a local collapse of the metric and the generation of a successive shell, if further energy is available. Such an observation will be useful later, when we prescribe a way to detect the separation surfaces without computing the entire field.

Before ending this section, we quickly introduce the equations studied in [17]. In a flat metric space, they read as follows:

$$\frac{\partial \mathbf{E}}{\partial t} = c^2 \text{curl} \mathbf{B} - \rho \mathbf{V} \quad (1.1)$$

$$\frac{\partial \mathbf{B}}{\partial t} = - \text{curl} \mathbf{E} \quad (1.2)$$

$$\text{div} \mathbf{B} = 0 \quad (1.3)$$

$$\rho \left( \frac{D\mathbf{V}}{Dt} + \mu (\mathbf{E} + \mathbf{V} \times \mathbf{B}) \right) = - \nabla p \quad (1.4)$$

with  $\rho = \text{div} \mathbf{E}$ , where  $\mathbf{E} = (E_1, E_2, E_3)$  is the standard electric field and  $\mathbf{B} = (B_1, B_2, B_3)$  the magnetic field. Moreover  $\mathbf{V} = (V_1, V_2, V_3)$  is a velocity field and the triplet  $(\mathbf{E}, \mathbf{B}, \mathbf{V})$  is right-handed. The given constant  $\mu$  is a charge divided by a mass. Both  $\rho$  (a kind of density) and  $p$  (a kind of pressure) may also take negative values. There is an additional “equation of state” relating  $p$  with the scalar curvature  $R$  of the space-time, however, for simplicity, we do not discuss this technical aspect here. There is also a perfect compatibility between the model equations and the request that the divergence of a suitable energy tensor (obtained as the sum of the standard electromagnetic stress tensor and a mass-type tensor with density  $\rho$ ) must be zero.

Free-waves are modelled by setting  $R = 0$ ,  $p = 0$ ,  $\frac{D}{Dt}\mathbf{V} = 0$  (rectilinear geodesics). In this way, equation (1.4) becomes:  $\mathbf{E} + \mathbf{V} \times \mathbf{B} = 0$ . Equation (1.1) turns out to be the Ampère law for a freely flowing unmaterial current with density  $\rho$  (actually, in this circumstance, the Lorentz acceleration  $\frac{D}{Dt}\mathbf{V}$  vanishes).

We recapitulate by saying that the evolution of electromagnetic phenomena (in principle of any kind) is governed by deterministic time-dependent equations (a nonlinear version of Maxwell's equations). The light rays can be interpreted as stream-lines of a fluid described by the non viscous Euler equations. These lines are associated with the geodesics of a space-time geometry. In synchronism, the geometry is perturbed by the passage of the wave. Therefore, every electromagnetic phenomenon is unavoidably related to a dynamical gravitational setting. The set of equations fulfills all the basic assumptions of invariance classically required in physics. Moreover, we could potentially build a model for describing matter by using exclusively electromagnetic waves.

This synthetic introduction may sound a little extravagant. Nevertheless, let us start with these pre-requisites to see if it is possible to translate these ideas in a mathematical language and provide alternative explanations to known facts, such as the Casimir effect.

## 2 Some quantitative results

According to the scenario depicted in the previous section, matter is made of massive subatomic particles only in small amount. The rest is electromagnetic energy organized by these particles to follow specific patterns. Due to its oscillating nature, such a background radiation is almost invisible, but it can be easily revealed through indirect experiments (for example, every time we observe photon emission, it means that a shell of a certain frequency has been released). The solution of the entire system of equations proposed in [17] should be able to provide all the necessary details to understand the structure of complicated molecular aggregations (for what concerns the evolution of the electromagnetic background, at least). Of course, this is quite an impressive amount of work, therefore, the search of a simplified model is a compulsory step.

For the applications we have in mind, it will be not necessary to know the exact evolution of the electromagnetic fields. It is sufficient instead to have an idea of the location and the size of the various shells and the frequency they carry. To this end, we will combine two hypothesis: the oscillating nature of the scalar electric potential and the inverse linear decay of the frequency rate as a function of the distance from the source.

We denote by  $\Phi$  the scalar electric potential and, as usual, we assume it satisfies the following wave equation:

$$\frac{1}{c^2} \frac{\partial^2 \Phi}{\partial t^2} = \Delta \Phi \tag{2.1}$$

where  $c$  denotes the speed of light.

We do not need to know exactly what is an electron (or a positive nucleus). We just assume that it is something with a diameter  $\delta > 0$  and imbedded in a sequence of spherical shells. Each shell is made of rotating photons, associated with a frequency:

$$\nu \approx \frac{c\beta}{r} \quad (2.2)$$

where  $r > \delta$  indicates the distance from the source and  $\beta$  is a given constant. In truth, the frequency should manifest a series of jumps, therefore, it is not a continuous function of  $r$  as indicated in (2.2). The problem is that, for the moment, we do not know the location of these jumps. By using the uniformly spherical expression (2.2), we also lose the notion of spin; however this is not a crucial aspect here.

According to the above hypotheses, we would like to get rid of the time variable in (2.1). If  $\Phi$  oscillates as  $\sin(\nu t)$ , we substitute the second derivative in time by:  $-\nu^2 \sin(\nu t)$ . Successively, we replace  $\nu$  by the expression in (2.2). These passages suggest to introduce a new function  $\tilde{\Phi}$ , that will be required to satisfy the stationary equation:

$$\Delta \tilde{\Phi} + \frac{\beta^2}{r^2} \tilde{\Phi} = 0 \quad (2.3)$$

It should be clear that there is no direct relation between  $\Phi$  and  $\tilde{\Phi}$ , since by applying the  $\Delta$  operator we did not compute the spatial derivatives of  $\nu$ . The equation (2.3) is however of primary importance for the discussion to follow.

We know that the gradient of the function  $\tilde{\Phi}$  is orthogonal to its level surfaces. If, in addition, these level surfaces consist entirely of stationary points, the vector  $\nabla \tilde{\Phi}$  is identically zero there. Roughly speaking, forgetting the time dependency, we have that that  $\nabla \Phi \approx \nabla \tilde{\Phi}$  is the electric field, and we would like to find, at least qualitatively, the surfaces where  $\nabla \Phi$  has no component orthogonal to the local tangent plane. As we said in section 1, these are transition surfaces between one shell and the next one.

The conclusions are heuristical but quite effective. For a given solution of (2.3), we compute the corresponding surfaces made of stationary points (as we shall see later, it will be simpler to compute the zeros). Then, we claim that, within a reasonable degree of approximation, these surfaces represent the boundaries of the different oscillating shells. Note instead that the behavior of  $\tilde{\Phi}$  between these surfaces has no physical meaning. Therefore, the technique we are going to explain is only finalized to find the location of the separation surfaces. This preliminary procedure will be then followed by other steps, with the scope to evaluating the global energy surrounding a piece of matter.

From the mathematical point of view, equation (2.3) is very peculiar. The operator  $\Delta$  is negative definite, so that there is a balance with the positive term  $(\beta/r)^2$ . The result is an indefinite, variable coefficients, Helmholtz problem. We observe that (2.3) admits self-similar solutions. As a matter of fact, a dilation

of the  $r$ -axis does not alter the nature of the equation, since  $\Delta$  behaves as  $1/r^2$ . This remark is important, because it will reveal a fractal underlying structure.

We can write the Laplacian in (2.3) in spherical coordinates. By looking for pure radial functions, after separation of variables, one obtains:

$$u'' + \frac{2}{r}u' + \frac{\beta^2}{r^2}u = 0 \quad (2.4)$$

admitting, up to multiplicative constants, solutions of the following form:

$$u(r) = \frac{1}{\sqrt{r}} \sin\left(\sqrt{\beta^2 - \frac{1}{4}} \log r\right) \quad \text{for } \beta > \frac{1}{2} \quad (2.5)$$

The above solution is an eigenfunction, corresponding to the zero eigenvalue, of the differential operator in (2.4). Another branch of solutions is obtained by replacing the sinus by the cosinus. Note that, by the substitution  $r \rightarrow re^\gamma$  with  $\gamma = \pi/\sqrt{\beta^2 - \frac{1}{4}}$ , we reobtain  $u$  up to a multiplicative constant.

Concerning boundary conditions, it is reasonable to assign the value of the electric field  $\nabla\Phi \approx \nabla\tilde{\Phi}$ . In terms of the function  $u$ , we can impose the value of its derivative at the point  $r = \delta$  and require that  $u \rightarrow 0$  for  $r \rightarrow +\infty$ . In alternative, one can follow the solution in (2.5) up to  $r = 0$ , discovering infinite oscillations.

Let us finally note that, since we are only interested to describe a qualitative behavior, it makes no difference to compute either the zeros or the stationary points of  $u$  (or the equivalent version with the cosinus). Due to the self-similarity properties of equation (2.4), these sets of points are interlaced and it will be sufficient to adjust the size of  $\delta$  to pass from one set to the other.

Therefore, let us compute for instance the zeros of (2.5). These are:

$$r_k = e^{\gamma k} \quad k \text{ integer}, \quad \text{with } \gamma = \frac{\pi}{\sqrt{\beta^2 - 1/4}} \quad (2.6)$$

implying that the amplitudes of the shells grow geometrically.

Once we have found the location of the transition boundaries, we should assign a frequency to each shell. Due to (2.2), this is done as follows:

$$\nu_k = \frac{c\beta}{r_{k+1}} \quad \forall r \in ]r_k, r_{k+1}] \quad (2.7)$$

where the index  $k$  can be also negative.

In addition, we would like to provide each shell with a suitable energy. Being a shell composed by photons of frequency  $\nu_k$ , it is customary to introduce a ground-state energy  $\mathcal{E}_k$  per unit of volume in order to satisfy the following relation:

$$\int \mathcal{E}_k dV = 4\pi \int_{r_k}^{r_{k+1}} \mathcal{E}_k r^2 dr = \frac{1}{2}h\nu_k \quad (2.8)$$

where  $h$  is the Planck constant. If  $\mathcal{E}_k$  is constant on the entire shell, we get:  $\mathcal{E}_k \approx 1/r_k^4 = e^{-4\gamma k}$ , which is quite a fast decay for  $k \rightarrow +\infty$ . Note that the computation of the integral of  $|\nabla\tilde{\Phi}|^2$  does not provide significant insight, since  $\tilde{\Phi}$  (determined up to multiplicative constant) is not the electric potential associated with the energy distribution in (2.8). We will also assume that there is a maximum frequency  $\nu_{\max} = c\beta/\delta$ , so that there exists a minimum index  $\hat{k}$  such that:

$$\nu_k < \nu_{\max} \quad \forall k > \hat{k} \quad (2.9)$$

If to the time-dependent electric field we sum up a stationary component  $q/(4\pi\epsilon_0 r^2)$ , for  $r > \delta$ , one can recover an interesting relation for the energy:

$$4\pi\epsilon_0 \int_{r_k}^{r_{k+1}} \left( \frac{q}{4\pi\epsilon_0 r^2} \right)^2 r^2 dr = \alpha \frac{e^\gamma - 1}{2\pi\beta} h\nu_k \quad (2.10)$$

where  $q$  is the electron charge and  $\alpha = q^2/2hc\epsilon_0$  is the fine structure constant. Thus, we got a well-known result: the energy in (2.10) is proportional to the Planck constant multiplied by the shell frequency. Note that this is not true with a general distribution of points  $r_k$ , but only when their growth is geometrical as in (2.6). Note also that the stationary potential  $\Phi_0 = -q/(4\pi\epsilon_0 r)$  is solution to the wave equation (2.1).

### 3 Organized energy patterns

It should be clear to the reader how important is the existence and the characterization of some extensive electromagnetic background, in order to explain the Casimir effect (see [6], [7]). We remind that this phenomenon concerns the attraction of two parallel uncharged metallic plates in vacuum. Thus, it would be worthwhile to recall first the official theoretical justification. This is based on the fact that some form of energy circulating at the exterior of the plates is larger than that trapped in between, resulting in a gradient of pressure pushing on the surfaces. The existence of the so called *zero-point* energy is something predicted by standard quantum mechanics (see, e.g., [11], [25], [19], [21], for a general overview). Such energy remains even when all the usual sources are removed from the system. It is a kind of fuzziness, attributed to matter, at a minimum uncertainty energy level, as a consequence of the Heisenberg principle. Its presence is however obscure in the classical non-quantum context.

The attractive force is relatively strong, since it behaves as  $d^{-4}$ , where  $d$  is the distance of the plates ( $d$  small enough). More precisely, denoting by  $A$  the area of the plates, for  $d \ll \sqrt{A}$ , the force is given by:

$$F = - \frac{hc\pi}{480 d^4} \quad (3.1)$$

In the theoretical analysis, the electromagnetic radiation around the plates is represented as an infinite sum of modes with averaged minimum energy. Then,



one observes that, since the plates are perfectly conducting and uncharged, in the space between them, only a subset of the modes has to be summed up. Thus, the difference of the outside and the inside energies is not zero, producing the Casimir effect. A nontrivial trouble is due to the fact that both the terms of the difference are divergent sums. This problem is generally overcome with mathematical arguments, not always clearly justified.

Our aim is twofold. First of all, we argue that the zero-point energy can be described deterministically, in terms of classical electrodynamics, via the equations introduced in [17]. Secondly, such an energy is finite, eliminating the inconvenience of handling divergent sums.

In order to proceed, we need to make some assumptions about the structure of a metallic surface  $\Omega$ . As we said in the previous section, electrons and nuclei carry, together with a stationary component providing for an effective charge, a system of electromagnetic shells vibrating at different frequencies. In the average, at a certain distance from  $\Omega$ , the charges compensate, so that we can get rid of the stationary part. We keep instead the oscillating component. If we are extremely close to the atoms, such a component is expected to display a very complicated evolution. But, as we move far from the molecular structure, one could simplify the setting and thinking of a sequence of plane parallel layers (neglecting unpredictable effects near the boundary of  $\Omega$ ), each one carrying a frequency that decays with the distance from  $\Omega$ . Note that the amplitude of the shells around the atoms grows geometrically (see (2.6)). Contrary to what would happen with a linear growth, the interference patterns, created by shell systems associated with different atoms, rapidly fade, giving rise to smooth flat parallel electromagnetic layers. In practice, we are assuming some symmetry properties of the molecular lattice, which might not be true in the case of nonconductive materials.

A way to model this behavior is to take equation (2.3), and substitute the distance  $r$  from a single particle with the distance  $x$  from  $\Omega$ :

$$\Delta\tilde{\Phi} + \frac{\beta^2}{x^2}\tilde{\Phi} = 0 \quad (3.2)$$

where  $\tilde{\Phi}$  depends on the variable  $x$  and the two variables  $y$  and  $z$ , extending on the plate surface. Although this is not a real restriction, let us suppose for simplicity that  $\Omega$  is a square. Now, if we use separation of variables, we arrive to:

$$u'' + \left(\frac{\beta^2}{x^2} - \lambda^2\right)u = 0 \quad (3.3)$$

Here  $\lambda$  is an eigenvalue of the 2-D Laplacian on the domain  $\Omega$ . Indeed, there are infinite eigenvalues, that can be related to the area  $A$  of  $\Omega$  in the following way:

$$\lambda = 2\pi\sqrt{\frac{n^2 + m^2}{A}} \quad n, m \text{ positive integers} \quad (3.4)$$

The corresponding eigenfunctions, depending on the variables  $y$  and  $z$ , have zero average in  $\Omega$ .

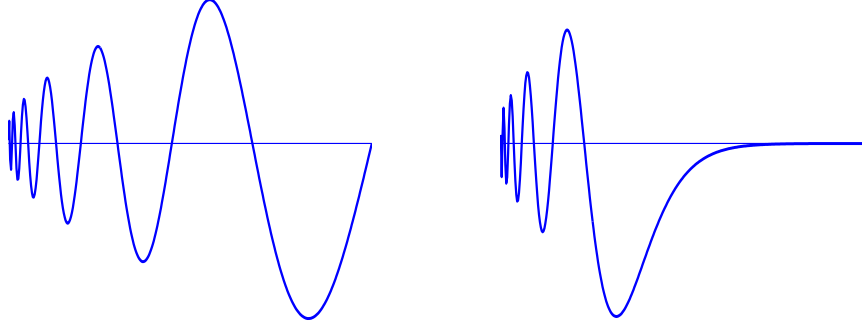


Figure 2: Solutions of the equation (3.3) for  $\lambda = 0$  and  $\lambda > 0$ .

According to the recipe illustrated in section 2, the successive step is to examine the distribution of the zeros  $x_k$  of  $u$ . To each interval we can then associate a frequency:

$$\nu_k = \frac{c\beta}{x_{k+1}} \quad \forall x \in ]x_k, x_{k+1}] \quad (3.5)$$

and a ground-state energy  $\mathcal{E}_k$  per unit of volume:

$$A \int_{x_k}^{x_{k+1}} \mathcal{E}_k dx = \frac{1}{2} h \nu_k \quad (3.6)$$

These computations are quite simple in the special case  $\lambda = 0$  (not included in (3.4)), where we can find an explicit solution of (3.3):

$$u = \sqrt{x} \sin\left(\sqrt{\beta^2 - \frac{1}{4}} \log x\right) \quad (3.7)$$

The plot of (3.7) is visible in the first picture of figure 2. Another solution is recovered by replacing the sinus by the cosinus. As we said, we are concerned with studying the behavior of zeros, minima and maxima, of the function  $u$ . For instance, by computing the zeros, we get:

$$x_k = e^{\gamma k} \quad k \text{ integer}, \quad \text{with } \gamma = \frac{\pi}{\sqrt{\beta^2 - 1/4}} \quad (3.8)$$

If  $\mathcal{E}_k$  is constant on the  $k$ -th shell, from (3.6) we obtain:

$$\mathcal{E}_k = \frac{ch\beta}{2A(1 - e^{-\gamma}) x_{k+1}^2} \quad (3.9)$$

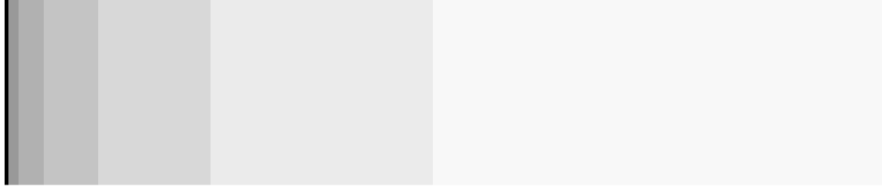


Figure 3: Stratification of electromagnetic layers outside a conductive surface ( $\lambda = 0$  in (3.3)). Each band is related to a complex evolutive framework of electromagnetic fields vibrating with a frequency that decays inversely with the distance from the plate.

The distribution of the various energy layers at the ground-state, is qualitatively illustrated in figure 3, by different scales of grey. With the distance the bands increase their width, but the energy levels reduce quite fast. Now, the sum of the total energy is finite, whenever  $\delta > 0$ . For  $\delta$  tending to zero the sum diverges, but this occurrence has no physical justification, since it means that we are not giving a sort of “granularity” to the molecular structure. In order to stay away from the plate, we define  $\nu_{\max} = c\beta/\delta$  and use only frequencies  $\nu_k$  satisfying (2.9).

The situation is a bit different when  $\lambda > 0$ . In this case, we do not have the explicit solution. However, some theoretical considerations can be made. One can check that, in the interval  $]\delta, +\infty[$ , there is only a finite number of zeros (see the second picture of figure 2). The last inflection point of the function  $u$  is for  $x = \beta/\lambda$ , followed by an exponential decay without oscillations. According to (3.4), when  $n = m = 1$ , there are no more zeros for  $x$  greater than  $\beta\sqrt{A}$ . A plot of the zeros and the energy levels is given in figure 4. Beyond the last zero, there is no appreciable energy. We recall that we are working at the minimum temperature, otherwise the situation would be rather different.

As a boundary condition we can require for instance that  $u(\delta) = 1$  (or  $u'(\delta) = 1$ , providing a qualitatively similar behavior). By the way, we can also impose  $u(\delta) = 1$  and  $u'(\delta) = 0$  at the same time. In this case  $u$  does not tend to zero for  $x \rightarrow +\infty$ , but grows exponentially. This behavior does not affect however the qualitative displacement of the zeros.

A rough evaluation of the zeros of  $u$  is obtained by rewriting (3.3) in the following way:

$$u'' + f^2 u = 0 \quad \text{with } f = \sqrt{\frac{\beta^2}{x^2} - \lambda^2} \quad (3.10)$$

for  $x < \beta/\lambda$ . We then integrate  $f$  with respect to  $x$  and find the values such that a primitive  $F$  is equal to  $k\pi$ , with  $k$  integer. These passages are not rigorously justified, but the idea is that  $u$  approximately behaves as the function  $\sin(F)$ .

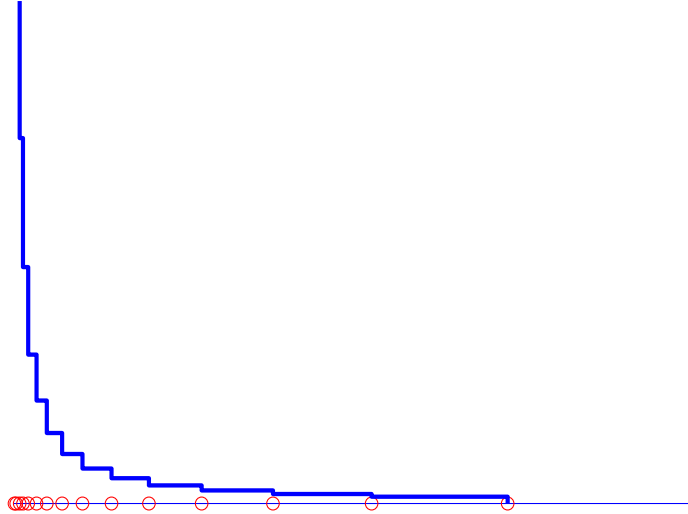


Figure 4: Energy levels of the layers associated to a conductive plate, for a given  $\lambda$  in (3.3). The dots are placed correspondingly to the zeros of  $u$ .

For example, with  $f$  defined as in (3.10), we have:

$$F = xf - \frac{1}{2}\beta \log \frac{\beta + xf}{\beta - xf} \quad \text{with } x < \frac{\beta}{\lambda} \quad (3.11)$$

The integration constant is such that  $F = 0$  when  $f = 0$ , and the function  $F$  turns out to be negative. When we compute the values such that  $F = k\pi$  ( $k$  negative integer), we get a sequence approaching zero with a behavior similar to that displayed by the zeros of  $u$  (see the dots of figure 4, which have been computed numerically by solving the differential equation). The number of these points is finite, when we are in the interval  $]\delta, \beta/\lambda[$ , for a positive  $\delta$ .

From the above arguments we can draw some conclusions. We are concerned with finding solutions  $\tilde{\Phi}$  of (3.2). We require that  $\tilde{\Phi}$  has zero average on the square plate  $\Omega$  and decays to zero far from  $\Omega$ . To this end, by separation of variables, we isolate the modes  $\sin ny$ ,  $\sin mz$ , transversal to  $\Omega$ , from the modes obtainable from the solution  $u$  of the single variable equation (3.3), with  $\lambda$  given in (3.4). Successively, for any fixed  $\lambda$ , we find the total ground-state energy  $\mathcal{E}_\lambda$ . This corresponds to a sum of suitable energy densities, carried by a sequence of independent layers parallel to  $\Omega$  (see figure 3). For  $\delta > 0$  (the “molecular rugosity” of the plate),  $\mathcal{E}_\lambda$  turns out to be finite.

The successive step is to compose the sum of the various  $\mathcal{E}_\lambda$ , with respect to the positive integers  $n$  and  $m$ . It is very interesting to observe that the electromagnetic parallel bands obtained for a certain  $\lambda_1$  are exactly distributed

as those obtained for another  $\lambda_2$ , after performing the linear transformation:  $x \rightarrow \lambda_1 x / \lambda_2$ . Once again, this reveals a fractal structure of the electromagnetic cloud circulating around the plate. As we said, the bands are comprised in the interval  $]\delta, \beta/\lambda[$ . Since  $\delta > 0$ , the integers  $n$  and  $m$  cannot be greater than a certain amount. This means that there is a finite number of terms  $\mathcal{E}_\lambda$ . Therefore, the global energy is finite. For  $\delta \rightarrow 0$ , one approaches the molecular structure of the metallic plate, which is made of an extraordinary large (but finite) number of atoms. The theory is coherent because, at molecular level, there is no need to take into account the modes with  $n$  and  $m$  larger than a given limit, so that the choice of a very small (but positive)  $\delta$  is well-suited to the circumstance. In our qualitative analysis, we have no practical suggestions about the magnitude of  $\delta$ . However, from the discussion above, it should be clear that its determination must be related to the interatomic distance (about one Ångstrom).

Thus, according to our model, the electromagnetic background, at its minimum energy level, is organized by a metallic body to form overlapped sequences of parallel films. Each sequence displays a geometrical growth and all the sequences can be transformed one into another by means of linear contractions. This construction may in part explain the fractal structure of matter (see for instance [23] or [30]). Our aggregations develop in the orthogonal direction to the surface and, more realistically, they are also time-dependent. It is not excluded that they may contribute to the formation of fractal stencils spread horizontally on the surface, as it is observed in a lot of applications, such as the analysis of fracture behavior. Fractal formations in the micro-world have been documented in a lot of circumstances, such as in the growth of electrochemical deposition. Among the numerous articles, we just mention a few papers: [2], [4], [24].

## 4 An explanation of the Casimir effect

The aim of the previous section was to show that the electromagnetic energy (always present, even at zero temperature), outside a piece of conductor, is distributed according to well-established patterns. Moreover, its total amount is finite. To explain the Casimir effect, we can now proceed with the usual arguments, that is, there is less energy trapped between two plates than outside.

In order to handle the case of two parallel plates at a distance  $d$ , we modify (3.3) as follows:

$$u'' + f^2 u = 0 \quad \text{with} \quad f = \sqrt{\beta^2 \left( \frac{1}{x^2} + \frac{1}{(d-x)^2} \right) - \lambda^2} \quad (4.1)$$

Now  $f$  is singular both for  $x = 0$  and  $x = d$ . The expression of  $\lambda$  is given in (3.4). The argument of the square root is positive when  $d$  is sufficiently small. To this purpose, for  $n = m = 1$ , the condition  $d < \beta\sqrt{A}$  is good enough. The other cases will be discussed later.

Other choices may be admissible for  $f$ , such as, for instance:

$$f = \sqrt{\beta^2 \left( \frac{1}{x} + \frac{1}{d-x} \right)^2 - \lambda^2} \quad \text{or} \quad f = \sqrt{\left( \beta \max \left\{ \frac{1}{x}, \frac{1}{d-x} \right\} \right)^2 - \lambda^2} \quad (4.2)$$

depending on how we measure the distance from the plates. They bring, more or less, to the same results.

Afterwards, we should compute the zeros  $x_k$  of  $u$  in the interval  $] \delta, d - \delta [$  and define the frequencies:

$$\nu_k = \begin{cases} c\beta \sqrt{(x_{k+1})^{-2} + (d - x_{k+1})^{-2}} & \forall x \in ]x_k, x_{k+1}[ \quad x_{k+1} \leq d/2 \\ c\beta \sqrt{(x_k)^{-2} + (d - x_k)^{-2}} & \forall x \in ]x_k, x_{k+1}[ \quad x_k \geq d/2 \end{cases} \quad (4.3)$$

which are an average of the frequencies induced by each plate separately. Again, we put a limit to  $\nu_k$  according to the inequality in (2.9). In practice, we will not consider the indices such that  $\nu_k \geq \nu_{\max}$ , in the global computation of the energy.

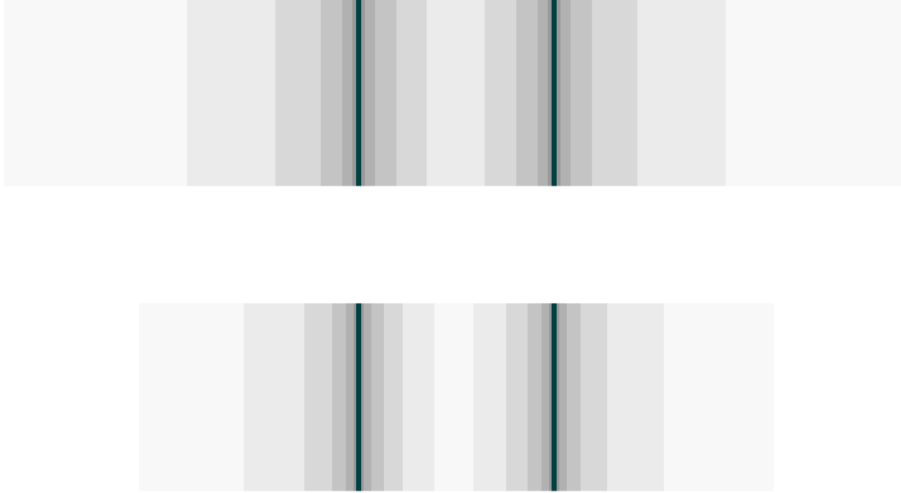


Figure 5: Stratification of electromagnetic layers between and outside two conductive surfaces at a given distance  $d$  (the vertical dimension is not in scale). The picture on top is related to a value of  $\lambda$  which is smaller than that corresponding to the picture on bottom. A fractal pattern is obtained by superimposing many pictures as the above ones, by varying  $\lambda$  in the range of the eigenvalues in (3.4).

We expect a distribution of the bands as in figure 5, where one can clearly notice a reduced energy in the central part. Now, we would like to quantify the missing contribution at the interior. Near the plates, independently of the side, the width of the bands is practically the same, i.e., the solutions of (3.3) and (4.1) behave in the same way. Therefore, we are interested to know the displacement of the zeros of  $u$  in (4.1) in the central part of the interval  $]0, d[$ .

For  $x \in ]\delta, d - \delta]$ , due to the fact that we now have two boundaries, we need to make additional assumptions. Actually, we would like to impose for instance  $u(\delta) = u(d - \delta) = 0$  (grounded plates), but these conditions produce in general only the trivial solution  $u \equiv 0$ . However, for certain values of  $d$ , the differential operator in (4.1) (whose sign is not definite) is allowed to admit eigenfunctions corresponding to the zero eigenvalue. Therefore, one can check that there is a sequence of values  $d$  such that problem (4.1) has nontrivial solutions even when  $u(\delta) = u(d - \delta) = 0$ . We claim that, in correspondence to these values, the set of layers is well-defined and somehow in equilibrium. For other choices of  $d$ , some layers (in particular the central ones) still do not possess the right energy to form a complete photon. In these unclear situations we are unable to predict, with strict accuracy, the size of the various bands. Nevertheless, we can argue as follows. Suppose that for a given  $d$ , we can find a nontrivial eigenfunction  $u$  and compute its zeros. Then, as  $d$  gets larger we obtain an intermediate situation where the global energy is going to be greater than the previous one. By increasing  $d$  again, further electromagnetic energy is captured between the plates, until we reach another stable configuration where  $u$  turns out to be the successive eigenfunction of (4.1). The new  $u$  displays more oscillations, and, for this reason, realizes a greater quantity of layers.

In figure 6, we see the plot of an eigenfunction  $u$ , obtained for a suitable value of  $d$ . In this case,  $u$  is an odd function vanishing for  $x = d/2$ . Therefore, together with the conditions  $u(\delta) = u(d - \delta) = 0$ , we also get  $u'(\delta) = u'(d - \delta)$ . In truth,  $u$  is determined up to a multiplicative constant, but, of course, this has no effect on the zeros. As we said before, the number of oscillations of  $u$  in  $] \delta, d - \delta [$  depends on the magnitude of  $d$ . Therefore, by slowly increasing the size of  $d$ , one can observe the transition from a state with  $n$  nodes to that with  $n + 2$  nodes, corresponding to the creation of a new central layer, through the absorption of a lower-frequency photon. A few steps of this evolution can be viewed in figure 7. The situation is very similar when we impose  $u(\delta) = u(d - \delta)$  (plates at the same potential) together with  $u'(\delta) = u'(d - \delta) = 0$  (uncharged plates). In this case the function  $u$  is even.

The detection of a quantized system of distances, realizing sets of completed shells (each shell carries the minimum allowed energy and there is no energy in excess to form a further shell), may explain the various states of excitation of an atom. As customary, the transition from one state to another is justified by the release or the absorption of photons. If this hypothesis is correct, one should be able to explain the origins of the quantized atomic structure. Numerical 3-D experiments are currently under way in order to understand if this guess is realistic.

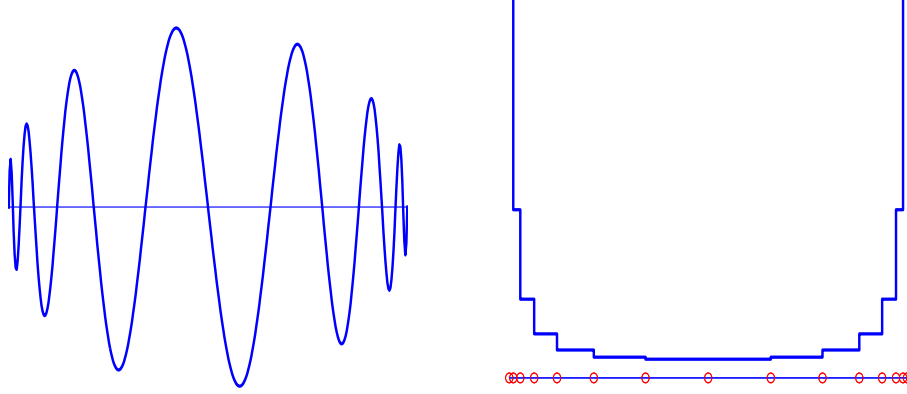


Figure 6: Qualitative plot of the function  $u$ , solution of (4.1), with  $u(\delta) = u(d-\delta) = 0$ , and the corresponding energy built on its zeros (represented by the dots).

We wish to show that the energy of the band in the middle (the one centered at  $x = d/2$ ) is proportional to  $d^{-2}$ . We can attempt a first approximate computation by taking  $\lambda = 0$  in (4.1) (note, for example, that  $\lambda$  is negligible when the plates are very close to each other). Afterwards, following the trick used in section 4, we evaluate a primitive of  $f$ :

$$F = \beta \left[ \sqrt{2} \operatorname{arcsinh}\left(\frac{2x}{d} - 1\right) + \operatorname{arctanh}\left(\frac{d-x}{\sqrt{d^2 - 2xd + 2x^2}}\right) - \operatorname{arctanh}\left(\frac{x}{\sqrt{d^2 - 2xd + 2x^2}}\right) \right] \quad (4.4)$$

and, successively, we compute the values  $x_k$  such that  $F = k\pi$ , where  $k$  is an integer.

For  $k = 0$  one has  $x_k = d/2$  and  $F(x_k) = 0$ . Hence, if we want to know what happens at the center of the interval  $]0, d[$ , we need to look at the distance  $|x_1 - x_{-1}|$ . Near  $x = d/2$ , in the first approximation, one can write:

$$F(x) \approx F\left(\frac{d}{2}\right) + F'\left(\frac{d}{2}\right)\left(x - \frac{d}{2}\right) = f\left(\frac{d}{2}\right)\left(x - \frac{d}{2}\right) = \beta\sqrt{2} \left(\frac{2}{d}x - 1\right)$$

Therefore, we get  $F(x) = \pi$  when  $x \approx \frac{1}{2}d(1 + \pi/\beta\sqrt{2})$ , which means that the quantity  $|x_1 - x_{-1}|$  is proportional to  $d$ .



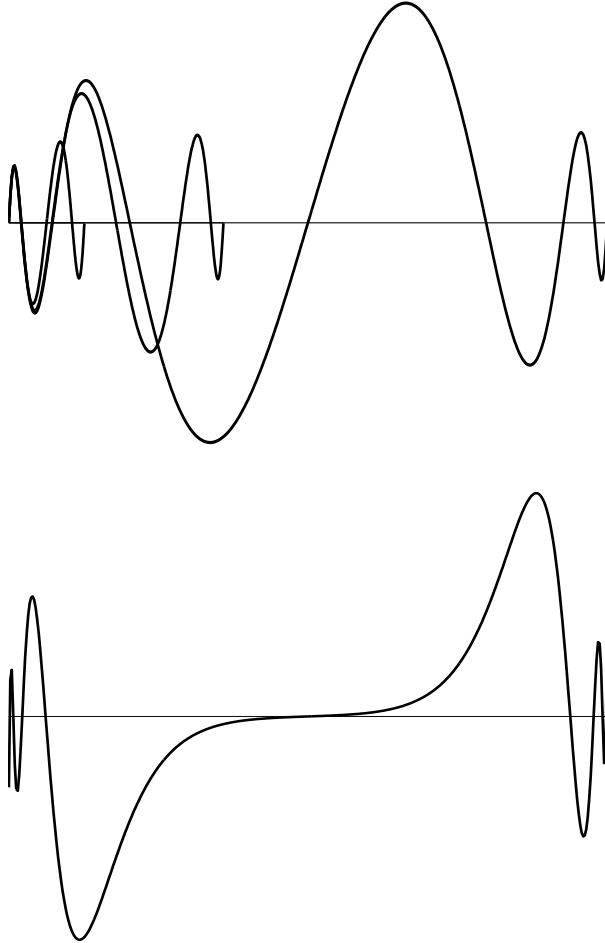


Figure 7: Solutions of (4.1) for different values of the parameter  $d$ . As  $d$  grows, more oscillations appear, until, depending on the ratio  $\beta/\lambda$ , one reaches a complete separation. In the picture on top the various  $u$  are actually eigenfunctions with zero boundary conditions. This is not true for the picture on bottom (not in the same scale-length as the above ones), because the plates are too far apart and the energy in the middle is too low to allow the formation of an entire photon.

Based on (4.3), the frequency in  $d/2$  is approximately  $\nu_{\text{central}} = 2c\beta/d$ , so that, using (3.6), as far as the the central band is concerned, the energy per unit of volume is:

$$\mathcal{E}_{\text{central}} = \frac{h\nu_{\text{central}}}{2A |x_1 - x_{-1}|} \approx \frac{K}{d^2} \quad (4.5)$$

where  $K$  is a constant.

Outside the plates, there are certainly more bands. Reasonably, the exceeding ones carry more than the energy  $\mathcal{E}_{\text{central}}$ . In addition, considering (3.9), let

us suppose that we can find  $k_0$  such that  $\mathcal{E}_{k_0} = \mathcal{E}_{\text{central}}$ . Then, due to the exponential growth of the nodes  $x_k$ , the sum  $\sum_{k=k_0}^{+\infty} \mathcal{E}_k$  is proportional to  $\mathcal{E}_{\text{central}}$  (use the relation:  $\sum_{m=m_0}^{+\infty} \sigma^m = \sigma^{m_0}/(1-\sigma)$ , valid for  $|\sigma| < 1$ ). Therefore, due to (4.5), the missing energy behaves as  $d^{-2}$ .

By differentiating the energy difference with respect to  $d$ , one gets that the force is proportional to  $-1/d^3$ . This result does not agree with formula (3.1). Nevertheless, we do not have to forget that the estimates obtained above, should be referred to a single specific choice of  $\lambda$ . Indeed, we have a multiplicity of layer structures, depending on the different values in (3.4). We recall that, by increasing  $\lambda$ , we produce a compression of the band range around the plates (see figure 5), that have a global extension within the interval  $[\delta, \beta/\lambda]$ .

The whole phenomenon is explained as follows. When the plates are far apart (at distance greater than  $\beta\sqrt{A}$ ), they are practically independent and no forces are exerted. As the distance is reduced, some central bands are eliminated by photon emission and an attractive force proportional to  $d^{-3}$  starts acting on the plates. The effect is due to the activation of the lowest transversal mode ( $n = m = 1$  in (3.4)). The other higher modes determine the presence of bands that are still not involved. As we further reduce the distance  $d$ , together with the elimination of some layers corresponding to the smallest  $\lambda$ , other layers (those for  $n, m \leq 2$ ) are successively discarded, increasing the strength of the force, becoming twice the previous one. Of course, the process is not continuous, but follows a quantized path. The emission of photons is subjected to complicated rules (we remind that there is a fractal structure underneath), so it might be not easily detected. Moreover, for simplicity, we threw away the time variable, but we do not have to forget that, in reality, the dynamics is extremely complex. Asymptotically, when  $d$  gets really small, the number of systems of layers involved is proportional to  $1/d$ . In fact, all the eigenvalues corresponding to  $\lambda < \beta/d$  ( $n = m \approx d^{-1}$ ) are associated with bands that are involved in the elimination process. Since the band systems are all similar (one can be mapped into another via a linear transformation), the total force is proportional to  $d^{-3}$  multiplied by  $d^{-1}$ , finally yielding (3.1). When  $d$  is close to  $\delta$  the plates are practically touching.

Our analysis reveals a non uniform spectrum of frequencies. Weighted spectra, mainly chosen according to statistics arguments and bringing to finite energy sums, may be introduced. A few papers dealing with this filtering procedure are for instance: [15], [16], [13]. The emission of photons, when the configuration of the plates is nonstationary, is a known phenomenon (see for instance [26] and [12]), often mentioned as dynamical Casimir effect. The present paper may help to clarify (also providing a mathematical model) the reasons for this amazing photon creation from vacuum. In [1], interesting connections linking the ‘‘critical states’’ in natural systems and the production of the so called *pink noise*, are made. We suspect that there is an analogy between the results in [1] and the states of equilibrium of the plates, corresponding to the eigenfunctions of problem (4.1), where  $\lambda$  is an eigenvalue related to the transversal modes. The relative movement of the plates passes through the emission of a complicated

sequence of photons exhibiting a well-determined spectrum of frequencies, that could be put in relation with some specific type of noise. However, the analysis of this aspect is out of the scopes of the present paper.

At the moment, little can be said concerning the proportionality constant in (3.1). The Planck constant and the speed of light are certainly involved, since they are used to set the energy levels at the ground-state. We do not advance any hypothesis concerning the values of  $\beta$  and  $\delta$ . The first one acts on the rate of growth of the layers, that follows a geometrical rule. The second one has effect on the global amount of energy. Some information could be recovered from the vast literature on power-law scaling for metals (see for example [22]).

This explanation of the Casimir effect may sound quite involved (on the other hand, the usual explanations looks rather simplistic), but agrees with an electrodynamic interpretation of the universe that could be spent to clarify many other facts, or, perhaps, to extract energy from the vacuum ([10], [3]).

## 5 Other configurations

We can now charge the two plates with opposite sign. Everybody would tell us that a stronger attraction is felt. But, how this phenomenon really happens? How can we justify the action at a distance of the Coulomb law? Our explanation is that the same identical layers, developing in the uncharged case, are also present in this case, transferring the information from one plate to the other. As argued in [17], the peculiar geometrical structure of the layers is decided by the time-dependent part of the electromagnetic fields (always existing, even at zero temperature), while the stationary part is just added to it. The stationary part emphasizes the negative pressure, resulting in a more pronounced suction effect.

In the vicinity of the plates the steady electric field is almost constant, and tends to zero far from them. As done for the treatment of the uncharged plates, by measuring the internal and the external energy densities  $\frac{1}{2}\epsilon_0|\mathbf{E}|^2$ , we come out with a resulting force pushing from outside, which is responsible for the attraction. Such a computation is trivial. However, here we are proposing an alternative viewpoint by arguing that the evaluation of the energy is not the integral of a continuous functions, but the sum of the partial contributions of the various layers. The terms of the sum combine the stationary field, with the time-dependent fields of the layers studied in the previous sections. If we are not at atomic scale, the second field is negligible with respect to the first one, so that the continuous stationary component dominates, masking the quantum effects.

Another issue we would like to discuss is the possibility of considering different geometrical assets of the plates. A typical example is the one of two spherical uncharged conductive plates at short distance  $d$ . The results about this case are controversial. From one side, with very technical arguments, in [5] it is shown that, surprisingly, the plates should repel, i.e., the inside zero-point energy is

greater than that outside. It seems however that there are no documented laboratory tests in favor of this hypothesis, mainly due to the difficulty of setting up the experiments. A general overview, together with a new approach to the theoretical treatment of hemispheric surfaces, are provided in [9] and [29]. In recent experiments (see [27], [20]), within the context of suitable geometrical environments at nanoscale level, the detection of repelling Casimir forces has been observed. Other extensions and a good list of references are provided for instance in [14].

From our viewpoint the situation is delicate. We recall that, according to our theory, the electromagnetic energy, pervading the universe from the very beginning, is organized, by the rapidly spinning particles inside a molecular texture, to follow well-determined patterns. This imprinting specifically depends on the type of material under study and its geometrical properties. As far as we are concerned, at the nanoscale, all the forces (Coulomb, van der Waals, Casimir, and even gravitational) are manifestation of the same modelling equations, combining in the appropriate manner (with a dosage depending on the context) electromagnetic phenomena with the space-time geometry, via Einstein's equation.

The case of the plane parallel metallic plates seems to be reasonably covered by the analysis developed here (provided we neglect what happens at their boundaries), because it displays strong symmetry properties. Nevertheless, we had to choose a minimum width  $\delta$  to give a bound to the infinitesimal fractal structure encountered when approaching matter (otherwise atoms would be indefinitely small). But, what happens when a plate is bent? On one side the molecular structure is stretched, on the other is compressed. In addition, this process may alter temperature. This means that, unless we have a very good knowledge of the behavior of matter at extremely short distances, it is hard to predict the shape of the electromagnetic layers circulating around. We also know that the innermost layers are those displaying the highest energy, influencing in this way the magnitude and the frequency of the successive layers. In the end, with some appropriate assumptions on the properties of matter, an analysis of the Casimir effect for spherical geometries (for instance) could be carried out with the help of equations (2.3) and (2.4). However, for the moment, this is an issue we would prefer to avoid.

## References

- [1] Bak P., Tang C., Wiesenfeld K. (1988), Self-organized criticality, Phys. Rev. A, **38**, pp. 364-374.
- [2] Barabási A. -L., Stanley H. E. (1995), *Fractal Concepts in Surface Growth*, Cambridge Univ. Press.
- [3] Bearden T., Bedini J. (2006), *Free Energy Generation, Circuits & Schematics*, Cheniere Press.

- [4] Bradley J. -C., Chen H. -M., Crawford J., Eckert J., Ernazarova K., Kurzeja T., Lin M., McGee M., Nadler W., Stephens S. G. (1997), Creating electrical contacts between metal particles using directed electrochemical growth, *Nature*, **389**, pp. 268-271.
- [5] Boyer T. H. (1968), Quantum electromagnetic zero-point energy of a conducting spherical shell and the Casimir model for a charged particle, *Phys. Rev.*, **174**, n. 5, pp. 1764-1776.
- [6] Casimir H. B. G. (1948), On the attraction between two perfectly conducting plates, *Proc. Kon. Nederland. Akad. Wetensch.*, **B51**, p. 793.
- [7] Casimir H. B. G., Polder D. (1948), The influence of retardation on the London-van der Waals forces, *Phys. Rev.*, **73**, pp. 360-372.
- [8] Chinosi C., Della Croce L., Funaro D., Rotating electromagnetic waves in toroid-shaped regions - part I, submitted.
- [9] Cho S. N. (2008), Is repulsive Casimir force physical?, arXiv:quant-ph/0408184v1
- [10] Cole D. C., Puthoff H. E. (1993), Extracting energy and heat from the vacuum, *Phys. Rev. E*, **48**, n. 2, pp. 1562-1565.
- [11] Dodd J. N. (1991), *Atoms and Light: Interactions*, Springer.
- [12] Dodonov V. V., Dodonov A. V. (2005), Quantum harmonic oscillator and nonstationary Casimir effect, *J. of Russian Laser Research*, **26**, n. 6, pp. 445-483.
- [13] Ellingsen S. A. (2008), Frequency spectrum of the Casimir force: interpretation and a paradox, *EPL*, **82**, 53001.
- [14] Farina C. (2006), The Casimir effect: some aspects, *Brazilian J. of Physics*, **36**, n. 4A, pp. 1137-1149.
- [15] Ford L. H. (1988), Spectrum of the Casimir effect, *Phys. Rev. D*, **38**, n. 2, pp. 528-532.
- [16] Ford L. H. (2007), Frequency spectra and probability distributions for quantum fluctuations, *Int. J. Theor. Phys.*, **46**, pp. 2218-2226.
- [17] Funaro D. (2008), *Electromagnetism and the Structure of Matter*, World Scientific, Singapore.
- [18] Funaro D. (2008), <http://cdm.unimo.it/home/matematica/funaro.daniele/phys.htm>
- [19] Ibison M., Haisch B. (1996), Quantum and classical statistics of the electromagnetic zero-point field, *Phys. Rev. A*, **54**, n. 4. pp. 2737-2744.

- [20] Lisanti M., Iannuzzi D., Capasso F. (2005), Observation of the skin-depth effect on the Casimir force between metallic surfaces, PNAS, **102**, n. 34, pp. 11989-11992.
- [21] Loudon R. (2000), *The Quantum Theory of Light*, Oxford Univ. Press.
- [22] Ma D., Stoica A. D., Wang X. -L. (2009), Power-law scaling and fractal nature of medium-range order in metallic glasses, Nature Materials, **8**, pp. 30-34.
- [23] Mandelbrot (1982), *The fractal Geometry of Nature*, Freeman, San Francisco.
- [24] Marani M., Banavar J. R., Caldarelli G., Maritan A., Rinaldo A. (1998), Stationary self-organized fractal structures in an open, dissipative electrical system, J. Phys. A: Math. Gen., **31**, L337.
- [25] Milonni P. W. (1993), *The Quantum Vacuum: an Introduction to Quantum Electrodynamics*, Academic Press.
- [26] Moore G. T. (1970), Quantum theory of the electromagnetic field in a variable-length one-dimensional cavity, J. Math. Phys., **11**, n. 9, p. 2679.
- [27] Munday J. N., Capasso F. (2007), Precision measurements of the Casimir-Lifshitz force in a fluid, Phys. Rev. A, **75**, 060102(R).
- [28] Munday J. N., Capasso F., Parsegian V. A. (2008), Measured long-range repulsive Casimir-Lifshitz forces, Nature, **457**, pp. 170-173.
- [29] Özcan M. (2005), Casimir energy between two concentric half spheres, Phys. Letters A, **344**, pp. 307-315.
- [30] Peitgen H. -O., Hartmut J., Dietmar S. (1992), *Chaos and Fractals, New Frontiers of Science*, Springer, New York.